PCCP

Cite this: *Phys. Chem. Chem. Phys.*, 2012, **14**, 6352–6358

www.rsc.org/pccp

PAPER

Photophysics of the galvinoxyl free radical revisited†

Jakob Grilj, Cedric Zonca, Latevi Max Lawson Daku and Eric Vauthey*

Received 14th November 2011, Accepted 6th January 2012
DOI: 10.1039/c2cp23577c

The photophysical properties of the free neutral radical galvinoxyl were studied by a combination of femtosecond time-resolved spectroscopy and quantum chemical calculations. The electronic absorption spectrum is dominated by an intense band at 430 nm that is ascribed to the $D_{9,10} \leftarrow D_0$ transitions. Upon photoexcitation at 400 nm, the population of the $D_{9,10}$ states decays within less than 200 fs to the electronic ground state. This ultrafast internal conversion does not involve intramolecular modes with large amplitude motion as the measured dynamics does not show any significant dependence on the environment, but is most probably facilitated by a high density of electronic states of different character. Depending on the solvent, a weak transient band due to the galvinoxylate anion is also observed. This closed-shell species, which is fluorescent although its deactivation is also dominated by non-radiative decay, is generated upon biphotonic ionization of the solvent and electron capture. The ultrashort excited-state lifetime of the galvinoxyl radical precludes photoinduced disproportionation previously claimed to be at the origin of the formation of both anion and cation.

Introduction

Galvinoxyl (Chart 1) is a free organic radical of outstanding chemical stability: it can be isolated in pure form and solutions are known to be stable even in the presence of oxygen.[1,2] This stability stems from both steric hindrance induced by the bulky *tert*-butyl groups and efficient delocalization of the unpaired electron all along the conjugated system. It is widely used as an EPR standard and serves as a radical scavenger/antioxidant, and, as such, it has numerous biological applications.[3,4] Since its discovery by G. Coppinger,[1] galvinoxyl and many of its derivatives have been studied extensively and electronic absorption,[5] photoelectron,[6] temperature dependent EPR spectra,[5,7,8] magnetic properties,[5,9,10] X-ray structure,[11,12] and photolysis experiments[13,14] have been published.

Galvinoxyl has a C_2 rotational symmetry axis in crystals.[11] The observed $C_{(ar)}$–CH–$C_{(ar)}$ bond angle at the methine carbon is 134° and the dihedral angle between the phenyl groups' planes is 12°. Overall, the molecule does not deviate greatly from planarity.[6] Delocalization of the unpaired electron over the whole aromatic system has also been evidenced in liquid solution *via* infrared[15] and EPR spectroscopy[16] and reproduced by quantum chemical calculations.[10]

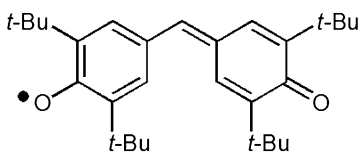

Chart 1 Galvinoxyl free radical.

The lowest energy transition observed in the electronic absorption spectrum is located at 860 nm (1.4 eV),[5] in agreement with CNDO/S quantum chemical calculations that found the lowest excited state at the same energy.[17] Galvinoxyl is a phenoxyl type radical and, apart from one publication[18] about the fluorescence of 2,4,6-tris(*tert*-butyl)phenoxyl radical that has been questioned later on,[19,20] no emission has been reported for this family of radicals. This is in contrast to, for example, the structurally similar diphenylmethyl type radicals, many of which emit around ~550 nm (2.3 eV) in room temperature solution.[19,21] The diphenylmethyl radical itself has a temperature-independent and remarkably long excited-state lifetime of 260 ns[22] and a high fluorescence quantum yield (Φ_f = 0.3).[23] This long lifetime is explained by the dipole forbidden character of the lowest transition reflected by a very low molar absorption coefficient.[21] Weir and co-workers found that the excited-state lifetime of differently substituted and isotopically labeled diphenylmethyl radicals correlates well with the D_1 state energy, as anticipated within the framework of the energy gap law.[24] Likewise, the ketyl radicals derived from benzophenone are known to fluoresce in liquid solution at 298 K.[19,25]

Benzyl type radicals are also fluorescent ($\lambda_f \approx 500$ nm), although only at low temperatures. The pronounced temperature effect on Φ_f originates from vibronic coupling between the D_1 and D_2 excited states, which offers an efficient non-radiative

Department of Physical Chemistry, University of Geneva, 30 quai Ernest-Ansermet, CH-1211, Geneva 4, Switzerland. E-mail: eric.vauthey@unige.ch

† Electronic supplementary information (ESI) available. See DOI: 10.1039/c2cp23577c

decay channel once enough vibrational energy is available.[19,22] Hence, the fluorescence lifetime at 77 K, where this channel is suppressed, amounts to 1.4 μs for the nπ D_1 excited state.[22]

The appearance of the anion and cation emission bands at λ_f = 590 and 560 nm, respectively, upon UV irradiation of solutions of galvinoxyl has been ascribed to photoinduced disproportionation.[13] Furthermore, a transient species with an absorbance maximum at ~580 nm observed in hexane and propanol solutions of galvinoxyl after UV excitation was ascribed to the excited state of galvinoxyl.[14] From these measurements, the lifetime of the D_1 state was estimated to be on the order of tens of microseconds,[14] an astonishingly high value considering that the D_1 state of galvinoxyl is, according to CNDO/S calculations, only 1.4 eV above its ground state.[17] On the other hand, such a long lifetime agrees well with the occurrence of photoinduced disproportionation, which, as it involves the diffusive encounter of two galvinoxyl molecules, is only possible if the D_1 state of galvinoxyl is sufficiently long-lived.

We report here on a joint experimental and theoretical investigation of the excited-state properties of galvinoxyl in solution, using a combination of ultrafast spectroscopy and quantum chemical calculations. Unlike closed-shell molecules, radicals are characterized by a high density of relatively low electronic excited states. In the case of the galvinoxyl radical, the calculations presented here indicate that optical excitation at 400 nm (3.1 eV) leads to the population of the D_9 or D_{10} state, a situation that is uncommon in closed shell molecules, where at most the second or third electronic excited state is reached at such excitation energies. We will show that, contrary to what has been previously reported, the excited-state lifetime of galvinoxyl is extremely short, in agreement with the high density of states, and with a lowest electronic excited state located only 0.9 eV above the ground state. Such a lifetime does not allow for the photoinduced disproportionation process previously suggested. The mechanism responsible for the formation of anion and cation will be discussed.

Experimental and computational details

Galvinoxyl (2,6-di-*tert*-butyl-α-(3,5-di-*tert*-butyl-4-oxo-2,5-cyclohexadien-1-ylidene)-*p*-tolyloxy free radical, also called Coppinger's radical) was purchased from Aldrich and used as received. The solvents acetonitrile (MeCN), ethanol (EtOH), methanol (MeOH), toluene and cyclohexane were of analytical grade, purchased from Aldrich and used without further purification. Absorption spectra in the UV/VIS spectral region were taken on a Cary 50 and in the NIR spectral region (up to 3000 nm) on a Cary 5000 spectrometer (Varian). Steady-state fluorescence was measured using a Cary Eclipse fluorimeter (Varian). The galvinoxyl radical samples for steady-state measurements had absorbances between 0.1 and 3 at 430 nm over 1 cm pathlength. Basic ethanol was obtained by adding 1% of aqueous NaOH solution to EtOH. The galvinoxylate anion samples had an absorbance of 0.8 at 580 nm since higher concentration improved chemical stability. Rhodamine B in ethanol (Φ_f = 0.7)[26] was used as reference to determine the fluorescence quantum yield.

The transient absorption (TA) setup has been described elsewhere.[27–29] Excitation was performed at 400 nm (for galvinoxyl; derived from the laser fundamental by frequency doubling) or 580 nm (for galvinoxylate; obtained using a home-built 2 stage non-collinear optical parametric amplifier) with *ca.* 2–3 mJ cm^{-2} pump energy (~1.5 μJ focused to 250 μm diameter) and spectral changes were monitored with white light pulses obtained by focusing weak 800 nm pulses into a CaF_2 window. The spectra were corrected for the chirp of the white light. The instrument response function (IRF) had a full width at half maximum (FWHM) of *ca.* 200 fs. The polarization of the pump was at the magic angle with respect to that of the probe pulses. The samples had an optical density around 0.2 at the excitation wavelength in the 1 mm pathlength cells used. During measurements, the sample solutions were agitated by nitrogen bubbling. No important sample degradation was observed as checked by steady-state absorption prior to and after the TA measurements.

At short times, when pump and probe laser pulse overlap, several non-linear effects can contribute to the measured signal, namely cross phase modulation (XPM), stimulated Raman and the coherent response. All but the latter can in principle be subtracted or singular value decomposition (SVD) can be used to separate them from the desired contribution resulting from a proper sequence of interactions with the pump and probe fields.[30,31] Subtraction requires precise positioning and low sample concentration since XPM is a non-linear process. SVD is known to be hampered by spectral shifts.[32] Because of these complications, we chose to perform a tail fit to the TA data ignoring those at time delays shorter than the width of the IRF. Obviously, this renders lifetimes of the order of the IRF inaccurate. The TA data have been analyzed by a multiexponential global fit and a target analysis.[32] The latter assumes successive reactions transforming one "species" into another following exponential kinetic rate equations: $A_1 \rightarrow A_2 \rightarrow A_3 \rightarrow A_4$. Such an analysis yields so called evolution associated difference spectra (EADS) which are linear combinations of the decay associated difference spectra obtained in a global multiexponential analysis.[32] The term evolution-associated is used to stress that EADS are related to spectral transformations that arise from either population dynamics (*e.g.* internal conversion) or vibrational and solvent relaxation. Since in the present case all these processes take place on the same time scale, it is in general not possible to unequivocally separate them and to assign a given EADS to a well-defined species.

Density function theory (DFT)[33,34] and time-dependent DFT (TDDFT)[35] have been used to characterize the isolated radical in the D_0 ground state. All calculations were performed with the ADF program package (ver. 2009),[36] using a large triple-ζ polarized (TZP) basis set from the ADF Slater-type orbital (STO) basis set database and were run unrestricted.[37] The ground-state geometry of galvinoxyl was thus optimized with the molecular symmetry constrained to C_2, with the 1s levels of the carbon and oxygen atoms frozen, and using the BLYP functional[38,39] augmented with the Grimme's semiempirical long-range dispersion correction (BLYP-D functional).[40] To analyze the ground-state absorption spectrum of galvinoxyl, a TDDFT electronic excitation calculation[35,41–43] was performed on the D_0 optimized geometry with the SAOP potential[44,45] and the TZP basis set, targeting the 40 lowest-lying excited states of

^{2}A and ^{2}B symmetry of the radical. No core level was frozen for the TDDFT calculation, which was performed within the adiabatic local density approximation.[35] Finally, as the D_0 and D_1 states of galvinoxyl are of ^{2}A and ^{2}B symmetry, respectively, the geometry of the galvinoxyl radical in the D_1 excited state was optimized by constraining the symmetry of the electronic state to ^{2}B and fixing the occupation numbers.[46]

Results and discussion

The BLYP-D/TZP optimized ground-state geometry of galvinoxyl is non-planar with a predicted angle of 15° between the two rings. This value agrees well with the experimental X-ray structure value of 12°.[11] The good agreement between experiment and theory actually extends to the whole structure, as attested for, for instance, by the similar values of the C=C–C bond angle at the methine carbon (calc. 134°, exp.[11] 132°) and those of the C–O bond length (calc. 1.254 Å, exp.[11,12] 1.20–1.27 Å).

The electronic absorption spectrum of the galvinoxyl radical in solution is shown in Fig. 1. This spectrum consists of an intense band around 430 nm and two weak bands at 770 and 860 nm. No other band could be distinguished at longer wavelength up to 3000 nm (data not shown). In MeCN and in basic EtOH solutions, an additional band not present in other solvents can be seen at 580 nm. The latter is not due to the galvinoxyl radical but arises from the galvinoxylate anion as discussed below. The TDDFT calculations performed with the galvinoxyl radical indicate that a high number of transitions of vanishing to very strong intensities contribute to this electronic absorption spectrum, as shown in Fig. 1. Table 1 summarizes the results of the electronic excitation calculation for the first 10 excited states D_n (n = 1,..., 10). They consist in the predicted energies and oscillator strengths of the $D_n \leftarrow D_0$ transitions, as well as their assignments based on the major monoelectronic excitation contributions and on the nature of the involved spin-up (α) or spin-down (β) Kohn–Sham spin-orbitals. Since the differences in the shapes and energies of the α and β Kohn–Sham spin-orbitals are very small (see Table 1 and Fig. S3 in the ESI†), we will adopt here, for the sake of simplicity, the common HOMO (which is singly occupied for a radical) and LUMO notation. The most relevant α and β orbitals and energies are given in the ESI.†

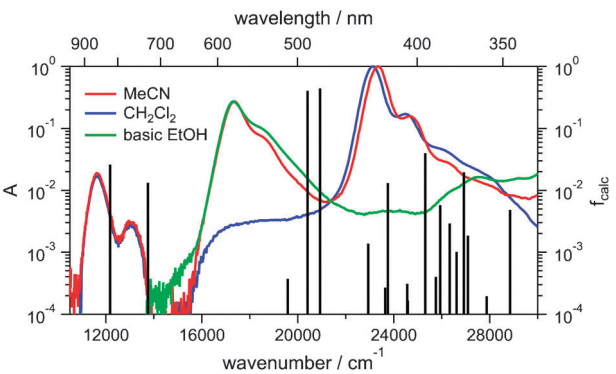

Fig. 1 Absorption spectrum of galvinoxyl in different solvents. The black bars indicate the calculated position and oscillator strength of the transitions.

The TDDFT calculations predict two electronic transitions lower in energy than that observed in the electronic absorption spectrum at 860 nm (Table 1). The corresponding D_1 and D_2 excited states are calculated at 1300 nm (0.9 eV) and 1200 nm (1.0 eV). These states have pure nπ character as they reduce each to a single monoelectronic excitation from one of the two β-spin-orbitals describing the oxygen lone pairs to the HOMO (Table 1). They are predicted to have a negligible oscillator strength, in agreement with their absence in the absorption spectrum. The calculated 0.9 eV energy of the first state contrasts with former CNDO/S calculations that located this nπ transition at 2 eV and that found the first electronic state to be a ππ transition at 1.4 eV.[17]

The first observable electronic absorption band at 860 nm (1.4 eV) is thus assigned to the $D_3 \leftarrow D_0$ transition. This band as well as that at 770 nm, that can be ascribed to the $D_4 \leftarrow D_0$ transition, both have ππ character. The intense absorption band measured at 430 nm (2.9 eV, $\varepsilon = 2{\cdot}10^5$ L mol^{-1} cm^{-1})[5,13] is found to be due to both $D_9 \leftarrow D_0$ and $D_{10} \leftarrow D_0$ transitions, which are predicted to occur at 2.5 eV (490 nm) and 2.6 eV (480 nm) and exhibit an admixture of nπ and ππ characters (Table 1 and Fig. 2).

The intense structured band with a maximum at 580 nm present in air saturated MeCN and basic EtOH can be ascribed to the galvinoxylate anion.[13,47] The mechanism

Table 1 Calculated transition energies E of galvinoxyl together with oscillator strength f. χ = main character (see also Table S1 in the ESI)

State		χ	Simplified MO ← MO transitions	Contribution (%)	E_{calc}/eV (nm)	$f_{calc} \times 10^4$	E_{exp}/eV (nm)
D_1	^{2}B	nπ	HOMO ← HOMO−1	100	0.929 (1300)	1	
D_2	^{2}A	nπ	HOMO ← HOMO−2	100	0.971 (1200)	0	
D_3	^{2}B	ππ	HOMO ← HOMO−3	66	1.509 (820)	261	1.4 (860)
		ππ*	LUMO ← HOMO	34			
D_4	^{2}A	ππ	HOMO ← HOMO−4	99	1.705 (730)	133	1.6 (770)
D_5	^{2}B	ππ	HOMO ← HOMO−5	99	1.705 (730)	34	
D_6	^{2}A	nπ*	LUMO ← HOMO−1	100	2.383 (520)	0	
D_7	^{2}B	nπ*	LUMO ← HOMO−2	100	2.427 (510)	4	
D_8	^{2}A	nπ*	LUMO ← HOMO−1	100	2.519 (490)	0	
D_9	^{2}B	ππ	LUMO ← HOMO	32	2.530 (490)	4045	2.9 (425)
		nπ*	LUMO ← HOMO−2	48			
		ππ	HOMO ← HOMO−3	16			
D_{10}	^{2}B	ππ*	LUMO ← HOMO	29	2.594 (480)	4405	3.0 (403)
		nπ*	LUMO ← HOMO−1	51			
		ππ	HOMO ← HOMO−3	15			

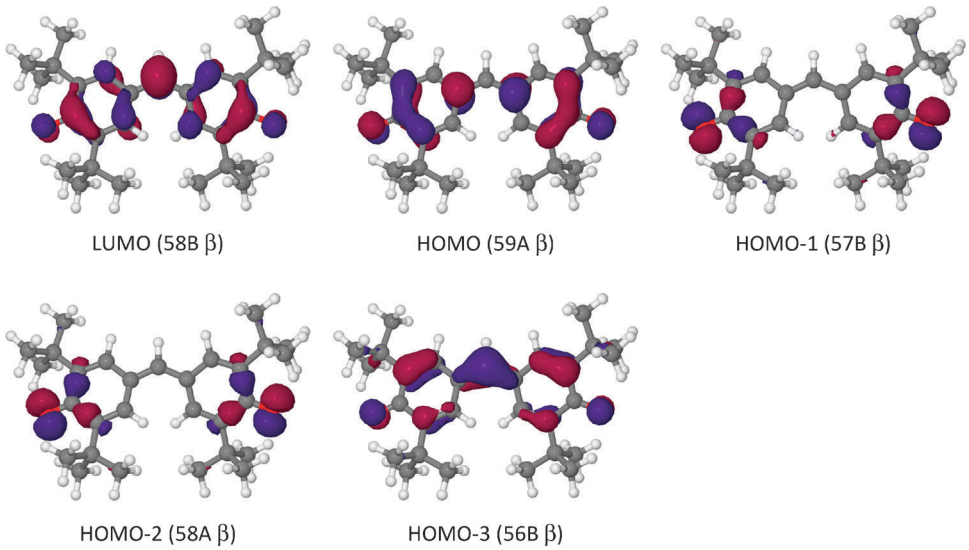

Fig. 2 Molecular orbitals involved in the most relevant electronic transitions of galvinoxyl. A larger set is given in the ESI.†

responsible for the formation of the anion in MeCN without the addition of a base is not clear, but this process only happens if oxygen is present in the solution. Although disproportionation is quite common for radicals, it seems quite improbable for galvinoxyl in view of its redox potentials (E^{red} = −0.07 V and E^{ox} = 2.2 V *vs.* SCE in MeCN).[48] The initially reported unreactivity of galvinoxyl against oxygen[1] was shown to stem from the inhibition of the oxidation reaction by hydrogalvinoxyl.[2,49] On the other hand, rapid reduction of galvinoxyl to the galvinoxylate anion in basic media is well documented.[47] Despite this, it seems justified to consider galvinoxyl to have an extraordinary stability.

Attempts to detect fluorescence from the galvinoxyl radical between 430 and 1100 nm were unsuccessful even in low temperature glasses (EtOH : MeOH = 1 : 1) and PMMA film. This lack of emission from an upper excited state is consistent with an ultrafast internal conversion to the D_1 state. We were not able to look for emission above 1100 nm, but the fluorescence quantum yield and the radiative rate constant of D_1 can be expected to be very small owing to its cubic dependence on the transition frequency, and the negligible $D_1 \rightarrow D_0$ transition dipole moment. Inspection of the molecular orbitals shows that the $D_1 \leftarrow D_0$ transition is associated with a charge transfer from the non-bonding oxygen lone pair to the π-system. This means that in the D_1 state, which results from the HOMO ← HOMO−1 excitation, the unpaired electron is more localized than in the ground state, namely at the oxygen atoms (HOMO−1 in Fig. 2).

Relaxing the geometry in ^{2}B symmetry, *i.e.* in the symmetry of the D_1 excited state, leads to minor structural changes as also concluded from resonance Raman measurements.[50] According to our calculations, the interplanar angle decreases by 3° and the C–O bond elongates by 2 pm, which can be understood by the transfer of an electron from a nonbonding orbital (with the node at the C atom) to the HOMO, which has a node between the C and O atoms (see Fig. 2).

Transient absorption (TA) spectra in various solvents were recorded after $D_{9,10} \leftarrow D_0$ excitation of the galvinoxyl radical at 400 nm (Fig. 3A). In all solvents used, the spectra are dominated by a negative band at 430 nm, the bleach signal stemming from the depletion of the ground-state population. This band is as narrow as the steady-state absorption band and does not hint on the presence of stimulated emission from the optically populated state. Additionally, two positive bands contribute to the TA spectra, one that is only present at early pump–probe time delays, and one that grows as time evolves at the expense of the former. Whereas the first TA band is weak and broad and covers essentially the whole observation window, the second one is narrow and located at the red edge

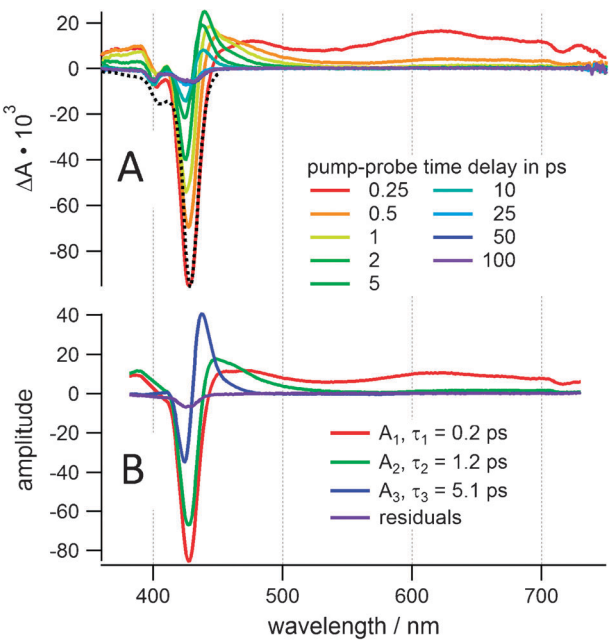

Fig. 3 Transient absorption spectra of galvinoxyl in MeCN at various pump–probe time delays (A) and evolution associated difference spectra obtained in a target analysis (B). The black dotted line represents the steady-state absorption spectrum.

of the intense bleach band, namely around 440 nm. This latter band decays in parallel to the bleach signal while shifting continuously to the blue. All these transient features decay almost to zero in less than 20 ps. The residual TA spectrum still contains about 5% of the initial bleach and, in MeOH, EtOH and toluene, it exhibits a small positive band with a maximum at 575 nm (better seen in Fig. S1 in the ESI†).

The time evolution of the TA spectra could be well reproduced by target analysis assuming a scheme with three successive first-order steps, $A_1 \rightarrow A_2 \rightarrow A_3 \rightarrow A_4$, the resulting evolution-associated difference spectra (EADS) being shown in Fig. 3(B). The shortest time constant, τ_1, is close to the IRF of the set-up and the EADS consists of the broad positive band and the strong negative bleach band. The second EADS exhibits only the narrow positive band on the red side of the bleach together with the negative band. However, the amplitude of the bleach band is smaller than in the first EADS, pointing to a partial recovery of the ground-state population in the $A_1 \rightarrow A_2$ step. In the third EADS, the positive band peaks at shorter wavelength, whereas the bleach is substantially smaller than in the second EADS, indicating a further recovery of the D_0 state population. As a consequence, the fastest component with τ_1 can be associated with the decay of an electronic excited state to the vibrationally hot electronic ground state, which then undergoes a biphasic vibrational relaxation with τ_2 and τ_3 to the thermally equilibrated ground state. Since excitation wavelength dependent TA measurements could not be performed owing to the low extinction coefficients of all but the 430 nm band, an identification of the electronic state responsible for the early TA spectra and reflected by A_1 in Fig. 3 is not possible. From the EADS, it is reasonable to ascribe A_1 to an electronic excited state but one cannot exclude that the D_1 state is never populated in the course of the electronic relaxation because of the presence of a conical intersection between higher excited states that could open a more efficient pathway toward D_0.

The EADS termed A_2 and A_3 show features that are typical of a vibrationally hot ground state, namely an ESA peaking on the red side of the ground-state bleach band and shifting continuously to the blue while decaying. Thus, A_2 and A_3 can be viewed as the vibrational hot ground state population at different stages of its relaxation toward thermal equilibrium. The first of these two time constants, τ_2, amounts to 1.2 ps independently of the solvent, pointing to intramolecular vibrational redistribution (IVR). Solvent independent IVR with time constants of some hundred fs has been reported for example for oxazine 720, nile blue and cresyl violet in solution.[51,52] Slower IVR could result from a small coupling between the vibrational modes excited in the internal conversion and the others. On the other hand, the other time constant associated with vibrational relaxation, τ_3, depends on the solvent and can thus be ascribed to vibrational cooling. However, τ_3 does not correlate with solvent properties such as viscosity, dielectric constant, heat capacity or thermal diffusivity.[53] The τ_3 values are close to those found with open-shell organic ions,[29] and in the range typical for medium sized organic molecules.[54]

Rapid sample degradation under irradiation with 400 nm pulses at high repetition rate (80 MHz) impeded reliable measurements of the D_9 state lifetime by fluorescence up-conversion spectroscopy. Since only minor photodegradation was observed in the aforementioned TA measurements (performed at 1 kHz laser repetition rate), the decomposition is most likely related to the excitation of an intermediate with a lifetime between some nanoseconds and microseconds. Indeed, the TA shows a long-lived residual that, in alcohols and toluene solution, resembles the transient reported by Kuzmin *et al.* in their flash photolysis experiment upon UV (260–380 nm) excitation.[14] Its absorption spectrum peaks at 575 nm (Fig. S1, ESI†), close to the 580 nm absorption maximum reported for the galvinoxylate anion. The same band has been detected in pulse radiolysis studies and was also ascribed to the anion.[55] We therefore conclude that the species observed in the flash photolysis studies[14] is the galvinoxylate anion and not the excited state of the galvinoxyl radical. In the present case, the galvinoxylate anion is most probably formed upon electron capture after multiphotonic ionization of the solvent. Indeed, the TA intensity at 575 nm in MeOH solution scales quadratically with the pump intensity (Fig. S2, ESI†), pointing to a mechanism that includes biphotonic ionization of the solvent at this excitation wavelength and subsequent trapping of the solvated electron by galvinoxyl in accord with the pulse radiolysis studies by Capellos and Allen.[55] Such a scheme explains why the highest galvinoxylate anion yield is observed in toluene and alcohol solutions, the solvents with the lowest liquid ionization potentials,[56] whereas no ionization takes place in MeCN which has a high ionization potential (Table 2).

Table 2 Lifetimes extracted from the transient absorption data (IRF 200 fs) in different solvents, and ionization potentials of the solvents

Solvent	τ_1/ps	τ_2/ps	τ_3/ps	IP_{liq}[a]/eV
Acetonitrile	0.18	1.2	5.1	12.2
Methanol	0.26	1.2	4.1	8.2
Ethanol	0.19	1.3	4.6	8.5
Cyclohexane	0.21	1.1	6.5	8.6
Toluene	0.13	1.3	5.9	6.8

[a] From ref. 56, 59 and 60.

In view of these results, the appearance of both galvinoxyl cation and anion after UV irradiation as reported by Ganyuk *et al.*[13] most probably originates from direct photoionization of the galvinoxyl radical, yielding the cation and a solvated electron which is then captured by another galvinoxyl to form the anion. Such a mechanism also explains why these authors did not observe the ions upon excitation in the 430 nm band. Considering the extremely short excited-state lifetime of galvinoxyl, a bimolecular photoinduced disproportionation reaction as proposed in ref. 13 is unfeasible at moderate concentrations. These authors detected the presence of the cation by its emission and not by its absorption, because of its relatively small absorbance. As a consequence, we cannot exclude the formation of the cation in our experiment upon direct multiphotonic ionization of the galvinoxyl radical.

The steady-state absorption and emission spectra of the galvinoxylate anion in basic ethanol solution are shown in Fig. 4. The presence of fluorescent impurities is responsible for the disagreement between the absorption and fluorescence excitation spectra and leads to a wavelength dependence of the fluorescence properties. According to TA measurements, the S_1 state lifetime of the galvinoxylate anion amounts to

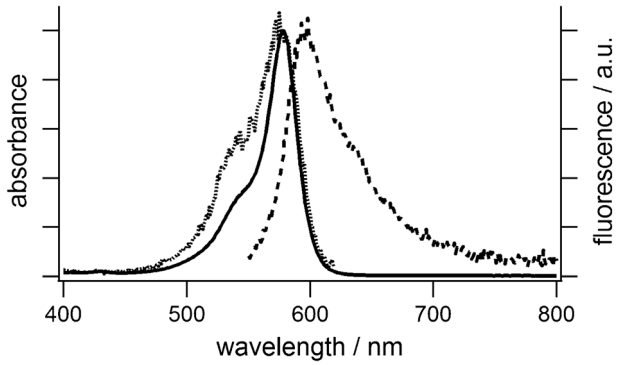

Fig. 4 Electronic absorption (solid line) and fluorescence emission (λ_{exc} = 540 nm) and excitation (λ_f = 630 nm) spectra of the galvinoxylate anion in basic ethanol. The poor agreement between absorption and excitation spectra and the wavelength dependence of the fluorescence spectra (not shown) stem from fluorescent impurities.

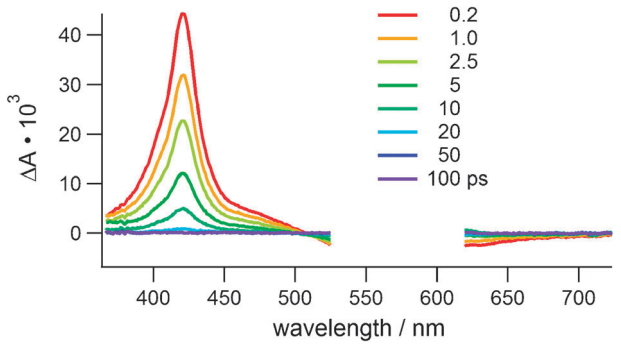

Fig. 5 Transient absorption spectra of the galvinoxylate anion in basic ethanol at various time delays after 580 nm excitation.

4 ps (Fig. 5). A radiative rate constant of $k_r = 2.0 \times 10^8$ s^{-1} was calculated from the steady-state spectra and the Strickler–Berg relation.[57] From this value and the measured fluorescence quantum yield of $\Phi_f = 10^{-3}$ (540 nm excitation), the excited state lifetime is predicted to amount to 14 ps, in good agreement with the experimental value of 4 ps. The excited-state lifetime of the closed-shell anion is also clearly governed by non-radiative relaxation processes. Whereas, a much slower non-radiative decay rate constant, (3 ns)$^{-1}$, is anticipated for the anion on the basis of the aforementioned energy gap law,[58] the D_1–D_0 energy gap of free radical is too small for this theory to be applied.

Summary and conclusions

Ultrafast internal conversion from $D_{9,10}$ to D_0 was found for the galvinoxyl free radical in all the solvents investigated. The corresponding release of 3 eV electronic energy in less than 200 fs is accomplished by a high density of states, that can be anticipated from the electronic absorption spectrum, and which were reproduced by the DFT calculations. The lowest lying excited state at 0.9 eV is of nπ character but extremely short lived contrary to that of benzyl type radicals, presumably due to the proximity of the ground and possibly of the D_2 state. Because of the remarkably high density of states below the optically populated state, the excited molecule benefits from very favorable Franck–Condon factors for non-radiative transitions to lower electronic states and/or does not need to distort much to reach a conical intersection between them. This strongly differs from those molecules with a large energy gap between the electronic states, which need substantial distortion to access a conical intersection to undergo very fast internal conversion.

After this ultrafast internal conversion, the D_0 state appears first vibrationally hot and relaxes in a bi-phasic fashion. As has been observed in other cases,[29] the first of the time constants associated with vibrational relaxation is solvent independent. Amounting to 1.2 ps, it is, however, much longer than what might be expected for intramolecular vibrational energy redistribution (IVR) of an organic molecule of this size in liquid solution where IVR time constants of a few tens or hundreds of femtoseconds are typical.[52] The insensitivity to solvent properties also makes an assignment of τ_2 to large amplitude structural changes unlikely.

Our results show that the long-lived transient that had been ascribed to galvinoxyl D_1 state[14] is in fact the galvinoxylate anion formed by electron capture after ionization, that can be induced by either UV or intense visible light. Furthermore, contrary to what was proposed in the literature,[13] photoinduced disproportionation of galvinoxyl is a highly improbable process and thus the observed presence of both cation and anion upon UV excitation is due to photoionization.

Acknowledgements

We thank Prof. Andreas Hauser for access to his Cary 5000 spectrometer. This work has been supported by the Swiss National Science Foundation through project No. 200020-124393.

References

1 G. M. Coppinger, *J. Am. Chem. Soc.*, 1957, **79**, 501.
2 E. R. Altwicker, *Chem. Rev.*, 1967, **67**, 475.
3 H. Shi, N. Noguchi and E. Niki, in *Flavonoids and Other Polyphenols*, ed. P. Lester, Academic Press, 2001, vol. 335, p. 157.
4 I. Nakanishi, K. Fukuhara, T. Shimada, K. Ohkubo, Y. Iizuka, K. Inami, M. Mochizuki, S. Urano, S. Itoh, N. Miyata and S. Fukuzumi, *J. Chem. Soc., Perkin Trans. 2*, 2002, 1520.
5 W. Gierke, W. Harrer, B. Kirste, H. Kurreck and J. Reusch, *Z. Naturforsch., B: Anorg. Chem., Org. Chem.*, 1976, **31**, 965.
6 I. Novak and B. Kovac, *Chem. Phys. Lett.*, 2005, **413**, 351.
7 K. Awaga, T. Sugano and M. Kinoshita, *Chem. Phys. Lett.*, 1987, **141**, 540.
8 G. Grampp, S. Landgraf, K. Rasmussen and S. Strauss, *Spectrochim. Acta, Part A*, 2002, **58**, 1219.
9 F. Dietz, N. Tyutyulkov and M. Baumgarten, *J. Phys. Chem. B*, 1998, **102**, 3912.
10 R. W. A. Havenith, G. A. de Wijs, J. J. Attema, N. Niermann, S. Speller and R. A. de Groot, *J. Phys. Chem. A*, 2008, **112**, 7734.
11 D. E. Williams, *Mol. Phys.*, 1969, **16**, 145.
12 H. S. Sheu, C. H. Lee, Y. Wang and L. Y. Chiang, *J. Chin. Chem. Soc.*, 1994, **41**, 797.
13 L. N. Ganyuk, N. F. Guba and V. D. Pokhodenko, *Theor. Exp. Chem.*, 1979, **14**, 421.
14 V. A. Kuzmin, I. V. Khudjakov and A. S. Tatikolov, *Chem. Phys. Lett.*, 1977, **49**, 495.
15 L. A. Kotorlenko, V. S. Aleksandrova and V. N. Yankovich, *J. Mol. Struct.*, 1984, **115**, 501.
16 W. Gierke, W. Harrer, H. Kurrek and J. Reusch, *Tetrahedron Lett.*, 1973, **14**, 3681.
17 L. S. Degtyarev, *Theor. Exp. Chem.*, 1988, **23**, 682.
18 T. Okamura and R. W. Yip, *Bull. Chem. Soc. Jpn.*, 1978, **51**, 937.
19 L. J. Johnston, *Chem. Rev.*, 1993, **93**, 251.

20 V. A. Smirnov and V. G. Plotnikov, *Russ. Chem. Rev.*, 1986, **55**, 929.
21 A. Bromberg, K. H. Schmidt and D. Meisel, *J. Am. Chem. Soc.*, 1985, **107**, 83.
22 D. Meisel, P. K. Das, G. L. Hug, K. Bhattacharyya and R. W. Fessenden, *J. Am. Chem. Soc.*, 1986, **108**, 4706.
23 D. Weir, *J. Phys. Chem.*, 1990, **94**, 5870.
24 D. Weir and J. C. Scaiano, *Chem. Phys. Lett.*, 1986, **128**, 156.
25 L. J. Johnston, D. J. Lougnot, V. Wintgens and J. C. Scaiano, *J. Am. Chem. Soc.*, 1988, **110**, 518.
26 F. Lopez-Arbeloa, P. Ruiz Ojeda and I. Lopez-Arbeloa, *J. Lumin.*, 1989, **44**, 105.
27 G. Duvanel, J. Grilj, A. Schuwey, A. Gossauer and E. Vauthey, *Photochem. Photobiol. Sci.*, 2007, **6**, 956.
28 N. Banerji, G. Duvanel, A. Perez-Velasco, S. Maity, N. Sakai, S. Matile and E. Vauthey, *J. Phys. Chem. A*, 2009, **113**, 8202.
29 J. Grilj, E. N. Laricheva, M. Olivucci and E. Vauthey, *Angew. Chem., Int. Ed.*, 2011, **50**, 4496.
30 S. A. Kovalenko, A. L. Dobryakov, J. Ruthmann and N. P. Ernsting, *Phys. Rev. A: At., Mol., Opt. Phys.*, 1999, **59**, 2369.
31 A. L. Dobryakov, S. A. Kovalenko and N. P. Ernsting, *J. Chem. Phys.*, 2005, **123**, 044502.
32 I. H. M. van Stokkum, D. S. Larsen and R. van Grondelle, *Biochim. Biophys. Acta, Bioenerg.*, 2004, **1657**, 82.
33 P. Hohenberg and W. Kohn, *Phys. Rev.*, 1964, **136**, B864.
34 W. Kohn and L. J. Sham, *Phys. Rev. A: At., Mol., Opt. Phys.*, 1965, **140**, 1133.
35 M. E. Casida, in *Recent Advances in Density Functional Methods Part I*, World Scientific Publishing, Singapore, 1995, vol. 1, p. 155.
36 G. te Velde, F. M. Bickelhaupt, E. J. Baerends, C. Fonseca Guerra, S. J. A. van Gisbergen, J. G. Snijders and T. Ziegler, *J. Comput. Chem.*, 2001, **22**, 931.
37 E. Van Lenthe and E. J. Baerends, *J. Comput. Chem.*, 2003, **24**, 1142.
38 A. D. Becke, *Phys. Rev. A: At., Mol., Opt. Phys.*, 1988, **38**, 3098.
39 C. Lee, W. Yang and R. G. Parr, *Phys. Rev. B: Condens. Matter Mater. Phys.*, 1988, **37**, 785.
40 S. Grimme, *J. Comput. Chem.*, 2006, **27**, 1787.
41 R. Bauernschmitt and R. Ahlrichs, *Chem. Phys. Lett.*, 1996, **256**, 454.
42 S. J. A. van Gisbergen, F. Kootstra, P. R. T. Schipper, O. V. Gritsenko, J. G. Snijders and E. J. Baerends, *Phys. Rev. A: At., Mol., Opt. Phys.*, 1998, **57**, 2556.
43 S. J. A. van Gisbergen, J. A. Groeneveld, A. Rosa, J. G. Snijders and E. J. Baerends, *J. Phys. Chem. A*, 1999, **103**, 6835.
44 O. V. Gritsenko, P. R. T. Schipper and E. J. Baerends, *Chem. Phys. Lett.*, 1999, **302**, 199.
45 P. R. T. Schipper, O. V. Gritsenko, S. J. A. van Gisbergen and E. J. Baerends, *J. Chem. Phys.*, 2000, **112**, 1344.
46 C.-L. Cheng, Q. Wu and T. Van Voorhis, *J. Chem. Phys.*, 2008, **129**, 124112.
47 M. S. Kharasch and B. S. Joshi, *J. Org. Chem.*, 1957, **22**, 1439.
48 A. Samanta, K. Bhattacharyya, P. K. Das, P. V. Kamat, D. Weir and G. L. Hug, *J. Phys. Chem.*, 1989, **93**, 3651.
49 F. D. Greene and W. Adam, *J. Org. Chem.*, 1963, **28**, 3550.
50 G. N. R. Tripathi, *Chem. Phys. Lett.*, 1981, **81**, 375.
51 A. M. Weiner and E. P. Ippen, *Chem. Phys. Lett.*, 1985, **114**, 456.
52 T. Elsaesser and W. Kaiser, *Annu. Rev. Phys. Chem.*, 1991, **42**, 83.
53 K. Iwata and H. Hamaguchi, *J. Mol. Liq.*, 1995, **65–66**, 417.
54 A. Pigliucci, G. Duvanel, L. M. L. Daku and E. Vauthey, *J. Phys. Chem. A*, 2007, **111**, 6135.
55 C. Capellos and A. O. Allen, *J. Phys. Chem.*, 1970, **74**, 840.
56 I. A. Shkrob, M. C. Sauer, A. D. Liu, R. A. Crowell and A. D. Trifunac, *J. Phys. Chem. A*, 1998, **102**, 4976.
57 S. J. Strickler and R. A. Berg, *J. Chem. Phys.*, 1962, **37**, 814.
58 W. Siebrand, *J. Chem. Phys.*, 1968, **49**, 1860.
59 C. Wu, Y. Xiong, Z. Gao, F. Kong, H. Lu, X. Yang and Z. Xu, *Chin. Sci. Bull.*, 2000, **45**, 1953.
60 S. H. Gong and A. Penzkofer, *Opt. Quantum Electron.*, 1999, **31**, 1145.

